- 1 Evaluating the feasibility of using downwind methods to quantify point source oil and gas emissions using continuous
- 2 monitoring fence-line sensors
- 3 Mercy Mbua\*,<sup>1</sup>, Stuart N. Riddick<sup>1,2</sup>, Elijah Kiplimo<sup>1</sup>, Kira B. Shonkwiler<sup>1</sup>, Anna Hodshire<sup>1</sup> and Daniel Zimmerle<sup>1</sup>
- <sup>1</sup>The Energy Institute, Colorado State University, CO, 80524, Fort Collins, USA
- <sup>2</sup>Department of Science, Engineering and Aviation, University of the Highlands and Islands Perth, Crieff Road, Perth,
- 6 PH1 2NX, UK

8

9

10

11

12

13

14

15

16

17

18

19

20

21

22

23

24

25

26

27

28

29

30

31

- 7 \*Correspondence to: Mercy Mbua (Mercy.Mbua@colostate.edu)
  - Abstract. The dependable reporting of methane (CH<sub>4</sub>) emissions from point sources, such as fugitive leaks from oil and gas infrastructure, is important for profit maximization (retaining more hydrocarbons), evaluating climate impacts, assessing CH<sub>4</sub> fees for regulatory programs, and validating CH<sub>4</sub> intensity in differentiated gas programs. Currently, there are disagreements between emissions reported by different quantification techniques for the same sources. It has been suggested that downwind CH<sub>4</sub> quantification methods using CH<sub>4</sub> measurements on the fence-line of production facilities could be used to generate emission estimates from oil and gas operations at the site level, but it is currently unclear how accurate the quantified emissions are. To investigate downwind methods' accuracy, this study uses fenceline simulated data collected during controlled release experiments as input for closed-path eddy covariance, aerodynamic flux gradient, the Gaussian plume inverse method, and the backward Lagrangian stochastic model in a range of atmospheric conditions. Generally, results show that flux quantification methods provide more reasonable estimates compared to point-source specific models especially when multiple releases are happening at the facility level. The closed-path eddy covariance quantified emissions with a mean relative factor (estimated emission over actual emission) of 0.7 to 1 for single-release single-point emissions, and within a mean relative of 1 and 2.4 for multirelease single-point emissions. The aerodynamic flux gradient method quantified emissions within a mean relative factor of 1.3 to 1.7 for single-release single-point emissions, and between 2.4 and 3.3 for multi-release single-point emissions. The Gaussian plume inverse model quantified emissions within a mean relative factor of between 2.4 and 2.6 for single-release single-point emissions, but largely overestimated emissions when multiple releases were happening; mean relative factor between 16 and 25. Similarly to the Gaussian plume inverse method, the backward Lagrangian stochastic model for point sources using WindTrax quantified within a mean relative factor of between 0.8 to 1 for single-release single-point emissions, but largely overestimated emissions for multi-release single-point emissions; mean relative factor of 3.9 and 11958. As continuous monitoring of oil and gas sites can involve complex emissions where plumes are not defined due to multiple sources, this study shows that common downwind point source dispersion models could largely overestimate emissions. This study recommends more testing of flux quantification models for oil and gas continuous monitoring quantification.
- 32 **Keywords:** Continuous monitoring; oil and gas; point source; closed-path eddy covariance; aerodynamic flux
- gradient; Gaussian plume inverse method; backward Lagrangian stochastic model

## 1 Introduction

Reducing methane (CH<sub>4</sub>) emissions from oil and gas systems is necessary for adhering to regulations and voluntary reporting frameworks such as the Oil & Gas Methane Partnership 2.0 (OGMP 2.0). The OGMP 2.0 provides a comprehensive measurement-based international reporting framework allowing companies to stay ahead of regulatory compliance requirements, meet investor and market pressure, have an enhanced corporate image, and prevent revenue loss by lowering their emissions. In the US, currently, the amount of CH<sub>4</sub> emitted from US oil and gas production are compiled by the US Environmental Protection Agency (EPA) under Subpart W. Typically, companies use a bottom-up inventory approach where emission factors (CH<sub>4</sub> emissions per equipment e.g., separator or emissions per event e.g., liquid unloading) are multiplied by activity factors (total number of pieces of equipment or events (OAR US EPA, 2023)) to generate emissions. This quantification approach has several shortcomings, including: 1. It separately calculates CH<sub>4</sub> emissions from natural gas and petroleum systems, which practically are not independent systems, and can result in bias based on changes in gas to oil ratios throughout a basin (Riddick et al., 2024a); 2. Some emission factors used are outdated (Riddick et al., 2024b) and others do not account for the temporal and spatial variation in emissions (Riddick and Mauzerall, 2023); and 3. Emission factors do not account for the longtail distributions (Riddick et al., 2024b). Recently, mechanistic models, such as the Mechanistic Air Emissions Simulator (MAES), have been developed to address shortcomings in bottom-up CH<sub>4</sub> reporting (Colorado State University, 2021), but these still depend on direct measurements to inform emission factors.

Top-down methods, including using aircraft such as Bridger Photonics LiDAR (Light Detection and Ranging; 90% detection limit of ~ 2 kg h<sup>-1</sup>) (Johnson et al., 2021) and satellites such as Carbon Mapper (predicted 90% detection limit of about 100 kg h<sup>-1</sup>) ("Carbon Mapper - Science & Technology," n.d.) can also be used to infer emissions. However, these survey methods only quantify emissions over a very short period of time (< 10 s) and observations are typically made during the day which can often coincide with maintenance activities that can bias emissions and result in overestimation (Riddick et al., 2024a; Zimmerle et al., 2024). Additionally, different top-down technologies measuring the same source have disagreed in their reported emissions which has called into question the credibility of these methods (Brown et al., 2023; Conrad et al., 2023). As a result, ensuring accuracy in models and technologies used in CH<sub>4</sub> emissions quantification has been a complex issue.

Currently, fence-line methods are used to detect, localize and quantify emissions. This approach uses point sensors fixed to the fence-line of the production site and emissions detected when the measured concentration exceeds a threshold, localized by triangulating multiple detections and quantified using a simple dispersion modelling framework, usually based on a Gaussian plume inverse approach (Bell et al., 2023; Day et al., 2024; Riddick et al., 2022a). The detection and localization of simulated fugitive emissions have been successful, with controlled release testing against point sensors and scanning/imaging solutions reporting a 90% probability of detection for emissions between 3.9 and 18.2 kg CH<sub>4</sub> h<sup>-1</sup> (Ilonze et al., 2024). Major shortcomings have been identified using a fence-line approach with quantified emissions reported at between a factor of 0.2 to 42 times for emissions between 0.1 and 1 kg CH<sub>4</sub> h<sup>-1</sup>, and between 0.08 and 18 times for emissions greater than 1 kg CH<sub>4</sub> h<sup>-1</sup> (Ilonze et al., 2024). As a result, questions have arisen if other approaches, such as the eddy covariance (EC) or aerodynamic flux gradient (AFG) would generate more accurate results. These methods have been suggested as they have been used to quantify

emissions from other sectors, i.e. agriculture (Denmead, 2008; Morin, 2019) and landfills (Xu et al., 2014), as well as to quantify emissions in large downwind areas (Vogel et al., 2024). Such quantification does not require assumptions made on downwind dispersion coefficients or micrometeorology that are often required for dispersion modelling (Denmead, 2008). Due to interest in using a subset of these methods to quantify emissions from oil and production sites, this study will evaluate the quantification accuracy of the closed-path EC, AFG, Gaussian plume inverse model (GPIM), and the backward Lagrangian stochastic model (bLs) for oil and gas point source quantification.

71

72

73

74

75

76

77

78

79

80

81

82

83

84

85

86

87

88

89

90

91

92

93

94

95

96

97

Eddy covariance is a vertical flux gradient measurement that measures CH<sub>4</sub> emissions based on the covariance between CH<sub>4</sub> concentrations measured using a fast-response analyzer (> 10 Hz) and vertical wind vector measured by a fast-response sonic anemometer (>10 Hz) (Figure 1A; Morin, 2019). It is typically implemented over long homogeneous fetches where eddy mixing scale is a small fraction of the distance from the site providing more predictable vertical transport. Dumortier et al., 2019 used EC to estimate known point source emissions at a cow's muzzle height and reported the model could estimate emissions between 90 and 113% of the true emission. Dumortier et al., 2019 stated the optimal controls for point source quantification and footprint modelling are using running mean, 15-minute averaging periods, no application of Foken and Wichura (1996) stationarity filter and use of the Kormann and Meixner (2001) footprint function. The study tested the model using an artificial CH<sub>4</sub> source at 0.8 m, programmed to emit when winds were coming from the source direction (± 45°), and when friction velocity (u\*) was above 0.13 m s<sup>-1</sup>. In Dumortier et al. (2019)'s point-source testing, they noted that amplitude resolution, skewness and kurtosis tests were disabled as they deleted almost all periods involving the artificial source in the footprint. Rey-Sanchez et al. (2022) studied the accuracy of Hsieh model (Hsieh et al., 2000), the Kljun model (Kljun et al., 2015) and the K & M model (Kormann and Meixner, 2001b) in calculating the footprint of point source hot spots using footprint-weighted flux maps. The study reported the K & M model to be the most accurate. Polonik et al. (2019) compared five gas analyzers, two open-paths, two enclosed-path and one closed-path analyzer for carbon dioxide EC measurements. The study noted that while open-path sensors minimize spectral attenuation and require smaller spectral correction factors compared to sensors with an inlet tube such as a closed-path sensor, open-path sensors risk data loss in non-ideal conditions like precipitation, fog, dust or dew. The main challenge of applying EC for continuous monitoring of oil and gas sites is instrument limitations (requires deployment of multiple sensors throughout a facility; sensor cost is a factor) and statistical tests as well as quality controls could filter out some of the data.

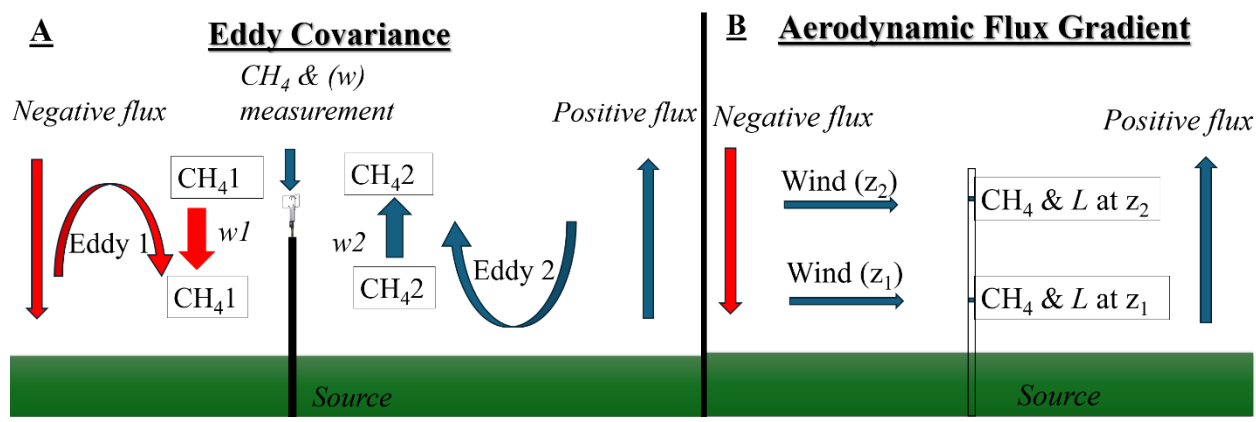


Figure 1: Illustrations of eddy covariance (A) and flux gradient measurements (B) where  $CH_4$  is methane concentrations, w is the vertical wind speed, L is the Monin-Obukhov length (measure of atmospheric stability), and z is the measurement height.

The AFG method quantifies CH<sub>4</sub> emissions from a source by comparing CH<sub>4</sub> concentrations at two heights (Figure 1B; Querino et al., 2011). Kamp et al. (2020) used the method to calculate ammonia fluxes over a grass field using a single analyzer by alternating two heights and reported 7% mean relative difference in flux in this approach compared to continuous measurements at two heights. Generally, the AFG approach is designed for homogeneous sources where footprints at different sensor heights would not affect quantification results, and its applicability to point source quantification, currently, is limited.

The GPIM method calculates CH<sub>4</sub> emission rate as a function of mole fraction at a point in space (x, y, z), downwind distance, perpendicular distance (crosswind), mean wind speed and atmospheric stability (Figure 2A; Riddick et al., 2022b). This method has been used to quantify emissions from oil and gas production sites especially for survey solutions (Riddick et al., 2022b). For a single point-source, Riddick et al. (2022b) reported absolute uncertainties of between 40.7 and 60%. Foster-Wittig et al. (2015) using controlled single point source tests reported average errors of between -5 to 6%. The limitations of the GPIM method are that it assumes a homogeneous emission source, steady-state flow, and uniform dispersion of gas in an open area free of obstructions (Hutchinson et al., 2017).

The bLs model adapted in WindTrax can simulate the transport of gases from point sources that emit them (Figure 2B; Crenna, 2006). The model releases individual particles and follows them along their unique path in air by mimicking random, turbulent motion of the atmosphere. Tagliaferri et al. (2023) investigated the validity of WindTrax in quantifying emissions from complex sources and reported the model to be reliable under neutral conditions, underestimated emission rates during unstable stratification and overestimated emissions during stable conditions. Similarly to the GPIM method, the model assumes free flow of air in the absence of obstructions and uses time-averaged data as input.

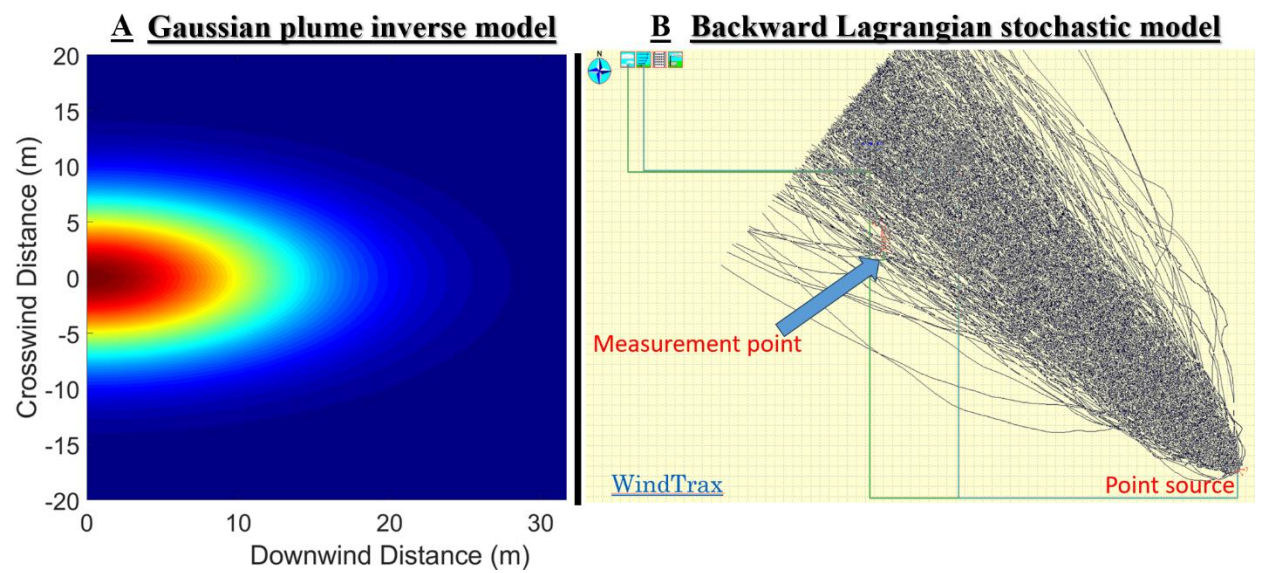


Figure 2. A: An illustration of a plume that follows a Gaussian plume inverse model where emission rate can be inferred from concentrations at different downwind distances and crosswind distances. B: An illustration of how the backward Lagrangian stochastic model traces particles to the source.

Continuous monitoring of CH<sub>4</sub> emissions using fence line sensors requires proper quantification of intermittent and persistent releases from oil and gas during all release (complex emission profiles) and atmospheric conditions (unstable, neutral and stable). Oil and gas emissions are characterized by intermittent, non-uniform, single or multiple point source emissions, varying in leak size, location, height and distance between the source and sensor, and are typically in complex aerodynamic environments (i.e. not flat). An ideal quantification model should always quantify emissions and should capture short and long-lasting emission events. Most models have been validated to work best during neutral conditions for single point sources. However, it is important to test and apply these models during non-neutral conditions as well as these are part of real-world conditions where continuous monitoring is applied. In this study, we evaluate if using a readily available CH<sub>4</sub> cavity ring down analyzer for models' quantification such as the closed-path EC is a feasible solution to quantify point source emissions.

This study aims to inform the feasibility of downwind quantification models in oil and gas settings by investigating which models are likely to work most of the time with instrumentation that is typically available for fence-line deployment. Fence-line sensor deployments involve multiple sensors, continuously running in all conditions and providing emissions data. Using robust releases and environmental conditions, this study aims to investigate the performance of these methods in quantifying emissions for known gas release rates and evaluating uncertainties that could result in incorrect CH<sub>4</sub> reporting. Specifically, the study will (1) evaluate the overall quantification accuracy of closed-path EC, AFG, bLs model, and the GPIM method in quantifying single-release single-point and multi-release single-point emissions that simulate oil and gas emissions, (2) determine the mean relative factor (estimated emissions over actual emission) for these models.

# 2 Methods

## 2.1 Experimental Setup

Controlled release experiments were conducted at the Colorado State University's Methane Emissions

Technology Evaluation Center (METEC) in Fort Collins, CO (USA, 65 miles north of Denver) between February 8, and March 20, 2024. The METEC center is a simulated oil and gas facility that does controlled testing for emissions leak detection and quantification technology development, field demonstration, leak detection protocol and best practices development (METEC, 2025). The weather conditions during the test period were mostly sunny but precipitation was also observed (32 sunny, 7 snowy, 12 rainy, 7 cloudy and 1 foggy day; Supplementary Information Section 1). Wind speeds were between 0 and 25 m s<sup>-1</sup> and temperatures ranged between -15 and +19 °C (Supplementary Information Section 1). Two stationary masts holding the instrumentation were setup on the North-West corner of METEC to take advantage of the predominant wind direction, avoid the largest aerodynamic obstructions and to simulate the likely placement of a fence-line instrument (Figure 3A; Day et al., 2024; Riddick et al., 2022a). Fence-line sensors are typically placed within the oil and gas perimeter (~30 m) (Riddick et al., 2022a). This study collected data for what we considered as close and far away releases; distances between 9 and 94 m.

Methane concentration data for closed-path EC, GPIM and bLs methods were collected through an inlet tubing (3.275 mm inner diameter) at 3 m height, connected to the ABB (Zurich, Switzerland) GLA131 Series Microportable Greenhouse Gas Analyzer (MGGA) set to sample at 10 Hz. The MGGA is a closed-path greenhouse gas analyzer with a ~3.2 lpm pump flowrate, 10 cm cell length, 1 inch cell diameter (~0.23 standard cubic centimeters per minute (sccm) effective volume), and 0.4 s gas flow response time. The inlet tubing was collocated with an R. M. Young (Traverse City, MI, USA) 81000 sonic anemometer (R.M. Young Company, 2023) which measured micrometeorology at 10 Hz (Figure 3-1). The northward, eastward and vertical separation of the inlet tubing from the sonic anemometer was 0, 0, -10 cm, respectively. For AFG, CH<sub>4</sub> concentration data was collected at 2 and 4 m using two Aeris (Hayward, CA, USA) MIRA Ultra Series analyzers connected to tubing with a 3.275 mm inner diameter (Figure 3-2). As we had only one sonic anemometer, data from the sonic anemometer collocated with the MGGA were used for the AFG quantification. The two sampling points are 9.4 m apart.

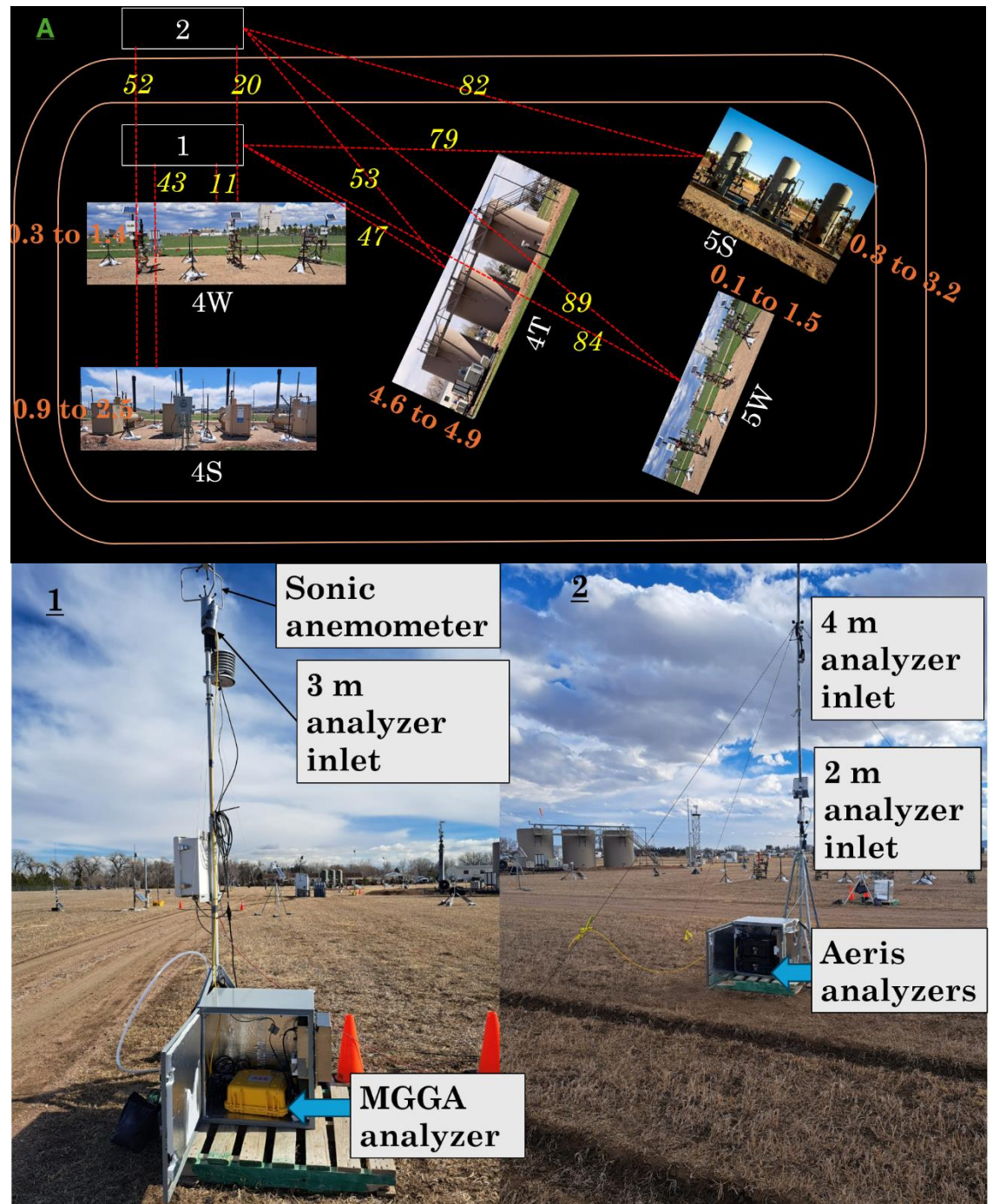


Figure 3: A: Map illustration of major pieces of equipment and the measurements points at Colorado State University's Methane Emissions Technology Evaluation Center (METEC) in Fort Collins, CO, USA. Equipment 4S denotes horizontal separators, 4W are well heads, 4T are tanks, 5S are vertical separators and 5W are well heads. The number 1 is the measurement point for the Microportable Greenhouse Gas Analyzer for closed-path eddy covariance, Gaussian plume inverse and backward Lagrangian stochastic model quantification. The inlet tubing and the sonic anemometer are at 3 m height. The number 2 is the measurement point for the Aeris analyzers at 2 and 4 m heights for aerodynamic flux gradient sampling. The red dotted lines with yellow numbers show the average distances (meters) between emission equipment and measurement point. The orange numbers show the range of emission heights (meters) for each equipment. The analyzers were hosted in a temperature-controlled box. The two sampling points are 9.4 m apart.

# 2.2 Controlled Methane Releases

 $\begin{array}{c} 171 \\ 172 \end{array}$ 

Controlled releases were part of the METEC Spring 2024 Advancing Development of Emissions Detection (ADED) Campaign conducted between February 6 and April 29, 2024 (Colorado State University, 2024). Natural gas of known CH<sub>4</sub> content was released from above-ground emission points attached to equipment typically present in an oil and gas facility (tanks, separators and well pads). The gas release rates ranged between 0.01 kg h<sup>-1</sup> and 8.7 kg h<sup>-1</sup>, and the release durations ranged from 10 seconds to 8 hours, simulating both fugitive and large emission events. The releases were run both during the day and night. The distance from the release points to the measurement points ranged between 9 and 94 m, and emission heights were between 0.1 and 4.9 m (Figure 3A). Emission points simulate the realistic size and locations of typical emissions from components such as the thief hatches, pressure relief valves, flanges, bradenheads, pressure transducers, Kimray valves and vents. The releases included both single-point emissions (single releases) and multi-point emission events (multiple simultaneous releases).

# 2.3 Calculation of Roughness Length

Surface roughness length (z0) was calculated from friction velocity (Supplementary Information Section 2a: Equations 1 and 2) by splitting the high frequency sonic anemometer data into 15-minute tables and filtering for those in neutral conditions, |L| > 500 (Supplementary Information Section 2a: Equation 3). The overall roughness length selected as the median of all the calculated z0 was 0.1 m (Rey-Sanchez et al., 2022).

### 2.4 Models Quantification

# 2.4.1 Eddy Covariance

### 2.4.1.1 Data pre-processing

Evaluating the MGGA CH<sub>4</sub> data showed that actual sampling was between 4 and 12 Hz (highest sampling at 6 Hz), even though it had been set to sample at 10 Hz (Supplementary Information Section 2b). To account for this sampling variability, data were filtered to when sampling was equal/greater than 8 Hz. Data where the frequency was greater than 8 Hz were down sampled to 8 Hz. The sonic anemometer meteorological data (horizontal wind vectors (u, v), vertical wind vector (w), temperature (T), and pressure (P)) actual sampling varied between 7 and 9 Hz with the most frequency at 8 Hz (Supplementary Information Section 2b). As the MGGA gas analyzer and sonic anemometer were not designed to clock synchronously, using the MGGA CH<sub>4</sub> clock time as a reference, meteorological data from the sonic anemometer were matched to the MGGA CH<sub>4</sub> data using linear interpolation to generate concentration-meteorological 8 Hz data.

The aggregated concentration-meteorological data were then merged with METEC's release data and metadata, and release event tables created. Release event tables were aggregated tables of concentration, meteorology and release (emission source location, duration and rate) information for all defined release events at METEC. The concentration-meteorological -release event data were then separated into single-release and multi-release events. Single-release events were when there was a single emission point at the site level, while multi-release events were when there was more than one emission point at the site level. The concentration-meteorological-release event tables were split into 5, 10 and 15-minute release event tables (i.e. there was a continuous release in the duration). Based on the bearing of the emission point to the measurement point and the average wind direction in the duration, the data was further filtered to downwind data,  $\pm 5^{\circ}$ ,  $\pm 10^{\circ}$ ,  $\pm 20^{\circ}$ , and  $\pm 45^{\circ}$ .

## 2.4.1.2 Flux calculation

Turbulent fluxes were calculated using the open software EddyPro® version 7 (LI-COR, Nebraska, USA, n.d.). Acquisition frequency was set at 8 Hz, while file duration and the flux interval were set at 5, 10, and 15 minutes, respectively, depending on the file being processed. Table 1 shows the instruments input to the software.

Table 1. Anemometer and Gas Analyzer Input into EddyPro

Anemometer Information		Gas Analyzer Information	
Model	81000	Model	Generic closed path
Height	3 m	Tube length	300 cm
Wind data format	u, v, w	Tube inner diameter	3.275 mm
North alignment		Nominal tube flow rate	3.2 l/m
North off-set	0.0	Northward separation	0.00 cm
Northward separation	Reference	Eastward separation	0.00 cm
Eastward separation	Reference	Vertical separation	-10.00 cm
Vertical separation	Reference	Longitudinal path length	10.00 cm
Longitudinal path length		Transversal path length	2.54 cm
Transversal path length		Time response	0.4 s

In raw data processing, axis rotations for tilt correction under wind speed measurement offsets was checked. Under turbulent fluctuations, double rotation and block average detrend methods were used. Covariance maximization with default was used for time lag detection; time lags detection was checked. Compensation for density fluctuations (Webb-Pearman-Leuning terms) was unchecked as the MGGA analyzer synchronously reported dry CH4 and water mole fractions, cell temperature and pressure. Mauder and Foken (2004) (0-1-2 system) were used for quality check. All statistical tests for raw data screening, Vickers and Mahrt (1997)— spike count/removal, amplitude resolution, drop-outs, absolute limits, skewness and kurtosis, discontinuities, time lags, angle of attack and steadiness of horizontal wind were checked. The default values for all these tests were used. Similarly, default settings for spectral analysis and corrections were used. Analytic correction of high-pass filtering effects (Moncrieff et al., 2005) for low frequency range; and correction of low-pass filtering effects (Fratini et al., 2012 - In situ analytic) and instruments separation (Horst and Lenschow, 2009 - only crosswind and vertical) in the high frequency range were used.

### 2.4.1.3 Post-processing

During post-processing, flux data were filtered based on (1) quality flags, Mauder and Foken (2004) (0-1-2 system), and (2) surface friction velocity ( $u^* > 0.13 \text{ m/s}$ ). Data that were flagged "2" were first filtered out as they were considered poor quality fluxes (LICOR, 2025), and the remaining dataset were filtered for high turbulence data. All data was filtered out as low quality and no further post-processing was done.

# 2.4.2 Aerodynamic Flux Gradient

Methane concentration data from the 2 and 4 m analyzers and meteorology data from the sonic anemometer were averaged to 1 Hz and then aggregated. Similarly to EC pre-processing, the aggregated concentration-

meteorological data were merged with METEC's release data and metadata, and release event tables created. The concentration-meteorological-release event data were then separated into single-release and multi-release events. For single-release events, the concentration-meteorological-release event tables were split into 5, 10 and 15-minute release event tables. Based on the bearing of the emission point to the measurement point and the average wind direction in the duration, the data was further filtered to downwind data,  $\pm 5^{\circ}$ ,  $\pm 10^{\circ}$ ,  $\pm 20^{\circ}$  and  $\pm 45^{\circ}$ . Multi-release events were further classified into multi-release single-point emissions (i.e., there were multiple emissions at the site level, but the mast was downwind of a single source) and multi-release multi-point emissions (i.e. there were multiple emissions at the site level and the mast was downwind of more than one source). As we were limited to data from a single source in single-release single-point emission and multi-release single-point scenarios. Flux determination and measurement footprint calculation are discussed in section 2.4.3. Methane flux (F, kg m<sup>-2</sup> s<sup>-1</sup>) were then calculated using the AFG equation (Supplementary Information Equation 6; Denmead, 2008; Kamp et al., 2020).

### 2.4.3 Footprints Calculation

Eddy covariance and AFG footprints were calculated using the Kljun et al. (2015) footprint model. Even though Rey-Sanchez et al. (2022) reported the Kljun et al. (2015) footprint model to be less accurate compared to the Kormann and Meixner (2001), Kormann and Meixner (2001) was too complex for our study because it required multiple sonic anemometers or tracer release experiments to calculate the exponential wind velocity power law, and the exponential eddy diffusivity power law for site specific data. Our study was limited to a single sonic anemometer, and this provided enough inputs for the Kljun et al. (2015) footprint model. The default pixel size 2 \* 2 m was used in this study. This study first calculated the area that contributed 90% of the vertical flux; and based on the location of the point source, the source was determined if it was within the 90% footprint area. Point source emissions of sources within this region were then calculated based on the approach by Dumortier et al. (2019). This approach assumes all measured flux is equal to flux resulting from a single point source. In case of the mast being downwind of more than one source, more sonic anemometers are needed to solve the two unknown point source fluxes.

# 2.4.4 Gaussian Plume Inverse Method

#### 2.4.4.1 Data pre-processing

Methane concentration data from the MGGA analyzer and meteorology data from the sonic anemometer were averaged to 1 Hz and pre-processed similarly to the AFG method. For continuous monitoring sensors, background concentration can be determined from CH<sub>4</sub> concentrations measured by a sensor upwind of the emission source, or by sampling when the wind is blowing away from the source. However, for continuous monitoring sensors, using an upwind sensor has the limitation of missing downwind background noise resulting from emissions in the preceding emission event where there is residual CH<sub>4</sub> in air especially during stable conditions, and capturing sensors drift in the downwind sensor. In this study, background CH<sub>4</sub> was calculated as the average of the lowest 5<sup>th</sup> percentile, 5 minutes before each release started. In cases where this background was greater than the mean CH<sub>4</sub> concentration in the quantifying duration, the minimum CH<sub>4</sub> concentration for that duration was used as the background. Methane enhancement was then calculated as CH<sub>4</sub> concentration minus the background.

## 2.4.4.2 Quantification

For single-release tables, the measurement point was downwind of a single source (single-release single-point emission), hence the tables were quantified as they were using the standard GPIM equation (Supplementary Information Section 2a: Equation 7). However, for multi-release events, the tables were further processed as the GPIM method is designed to quantify a single point source at a time. For multi-release events, the number of emission points in the downwind tables were used to further classify the tables into multi-release single-point emissions (i.e. there were multiple emissions at the site level, but the mast was downwind of a single source), and multi-release multi-point emissions (i.e. there were multiple emissions at the site level and the mast was downwind of more than one emission source). The GPIM method was only used for multi-release single-point emissions.

### 2.4.5 Backward Lagrangian stochastic model

Pre-processed data from the GPIM method was used for bLs quantification. Quantification was done using the open-source software WindTrax 2.0 (Crenna, 2006; WindTrax 2.0, n.d.). For every 5-, 10- and 15-minute duration in the  $\pm 5^{\circ}$ ,  $\pm 10^{\circ}$ , and  $\pm 20^{\circ}$ , respectively, inputs included roughness length (z0), Monin-Obukhov length (L), mean (wind speed, wind direction, concentration, pressure, temperature), background concentration, source height, and distance from the emission point to sensor. WindTrax is also designed to quantify a single point source at a time, and hence, was only used to quantify single-point single emissions and multi-point single emissions.

- 3 Results
- 3.1Eddy Covariance

# 3.1.1 Single-Release Single-Point

For single-release single-point (SRSP) emissions, the closed-path EC quantified emissions correctly within a mean relative factor (MRF) of between 0.67 and 0.97 at  $\pm 45^{\circ}$  wind sector range (Figure 4). The MRF was 0.97, 0.67 and 0.77 for a 97, 41 and 28 sample size at an averaging period of 5, 10 and 15 minutes, respectively (Figure 4). At  $\pm 5^{\circ}$  wind sector range, the sample size was 1, 2 and 3 at 5, 10 and 15-minutes averaging periods, hence, no reasonable quantification results (Supplementary Information Section 3.1.1). At  $\pm 10^{\circ}$  wind sector range, the MRF was 0.60, 0.95, and 1.71 for a 15, 6 and 6 sample size, at averaging periods of 5, 10 and 15-minutes, respectively (Supplementary Information Section 3.1.1). At  $\pm 20^{\circ}$  wind sector range, the MRF was 0.53, 0.86, and 1.10 for a 40, 16 and 14 sample size, at averaging periods of 5, 10 and 15-minutes, respectively (Supplementary Information Section 3.1.1).

# $\frac{Eddy\ Covariance}{Single-Release\ Single-Point\ -\ \pm 45^{\circ}}$

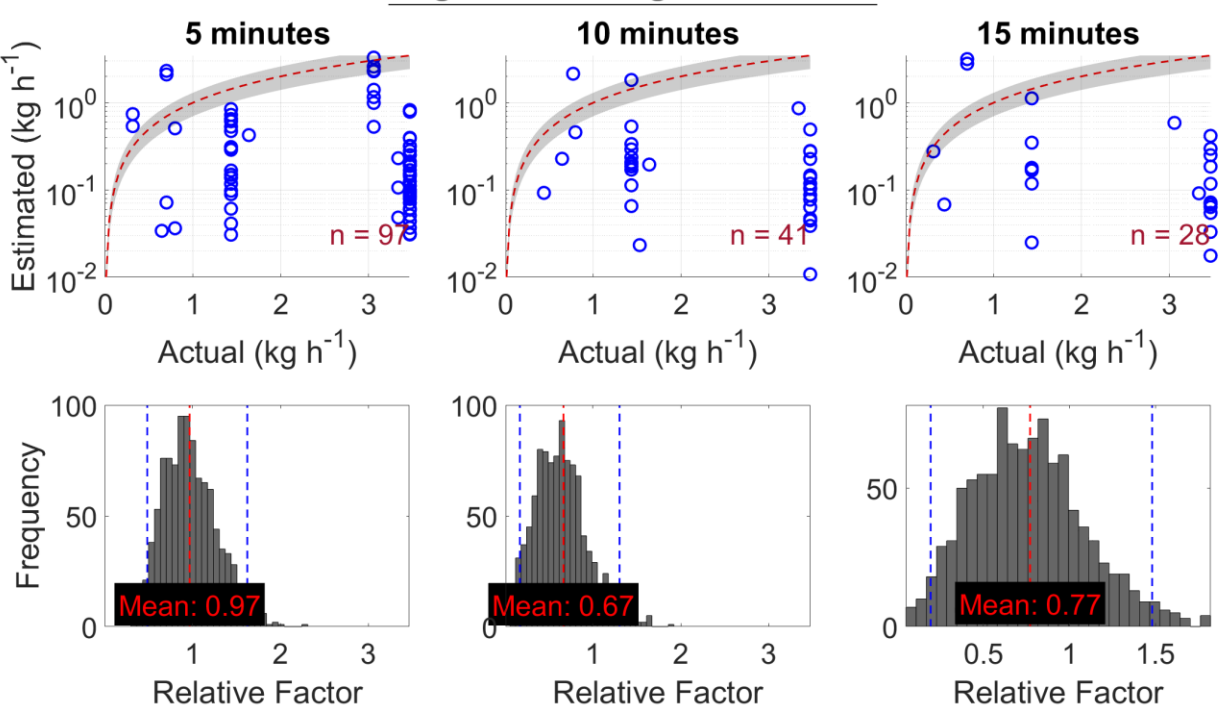


Figure 4. Top plot: Estimated emission vs actual emission (kg h<sup>-1</sup>) for a single-release single-point at site level,  $\pm 45^{\circ}$  wind sector range. The red dotted line is a 1:1 line based on actual emissions i.e. points below the line are underestimated and above are overestimated emissions. The gray region represents  $\pm 30\%$  of the actual emission. The sample size is n. Bottom plot: A bootstrap of mean relative factor (MRF: estimated emissions divided by actual controlled emission) for a single-release single-point,  $\pm 45^{\circ}$  wind sector range. An MRF of less than 1 shows an overall underestimation of emissions while an MRF of greater than 1 shows an overall overestimation of emissions. The dotted blue lines are the lower confidence intervals (CI) and upper CI, 95% confidence intervals.

# 3.1.2 Multi-Release Single-Point

For multi-release single-point (MRSP) emissions, the closed-path EC quantified emissions correctly within an MRF of between 1.02 and 2.43 at  $\pm 45^{\circ}$  wind sector range (Figure 5). The MRF was 1.02, 2.43 and 1.88, for a 355, 183, and 110 sample size at an averaging period of 5, 10 and 15 minutes, respectively (Figure 5). At  $\pm 5^{\circ}$  wind sector range, the MRF was 1.68, 5.21 and 5.16 for a 61, 34 and 23 sample size, at averaging periods of 5, 10 and 15-minutes, respectively (Supplementary Information Section 3.1.2). At  $\pm 10^{\circ}$  wind sector range, the MRF was 2.75, 3.32, and 4.11 for a 124, 70 and 44 sample size, averaging periods of 5, 10 and 15-minutes, respectively (Supplementary Information Section 3.1.2). At  $\pm 20^{\circ}$  wind sector range, the MRF 2.08, 2.89 and 2.70 for a 284, 143 and 80 sample size, at averaging periods of 5, 10 and 15-minutes, respectively (Supplementary Information Section 3.1.2).

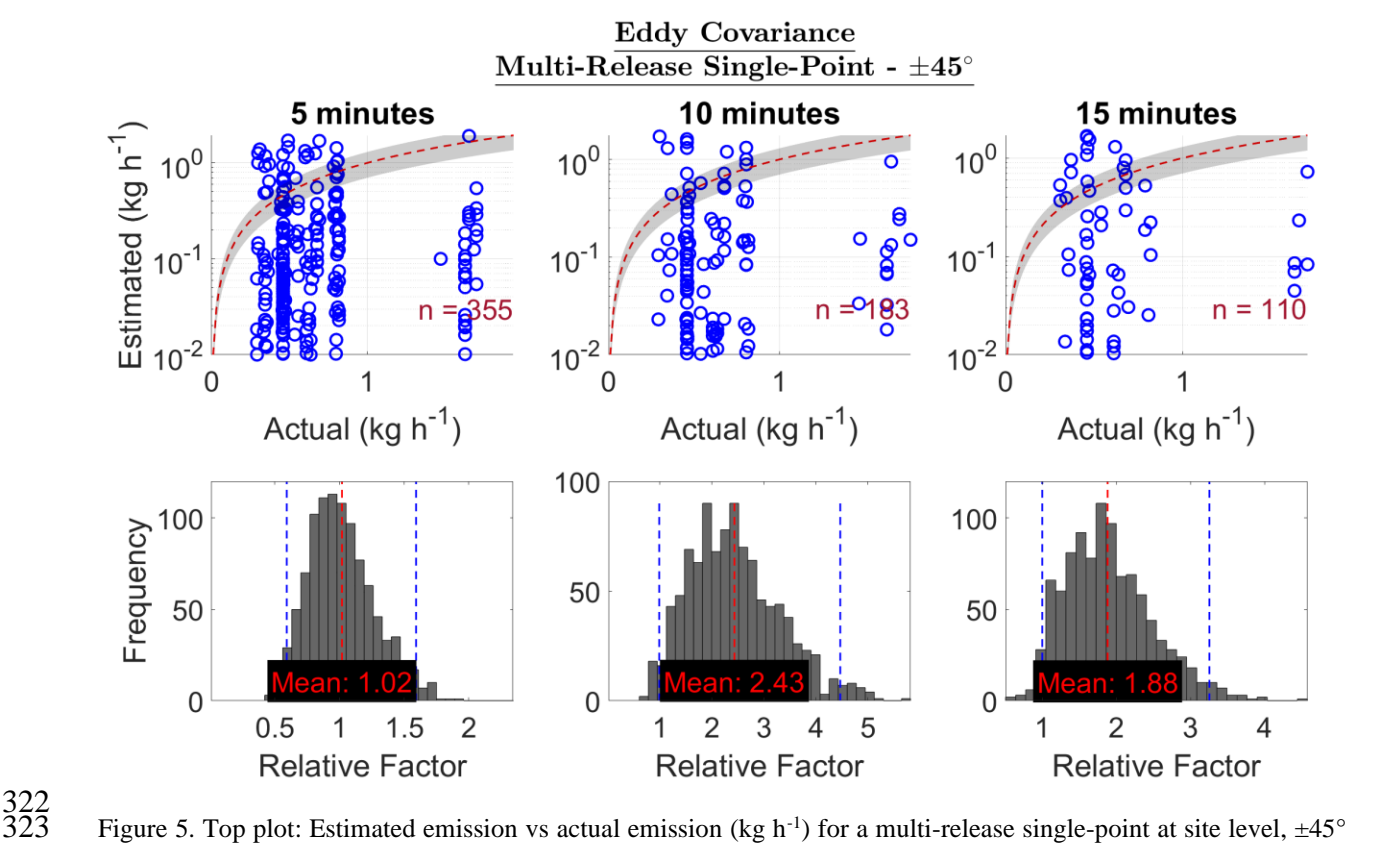


Figure 5. Top plot: Estimated emission vs actual emission (kg h $^{-1}$ ) for a multi-release single-point at site level,  $\pm 45^{\circ}$  wind sector range. The red dotted line is a 1:1 line based on actual emissions i.e. points below the line are underestimated and above are overestimated emissions. The gray region represents  $\pm 30\%$  of the actual emission. The sample size is n. Bottom plot: A bootstrap of mean relative factor (MRF: estimated emissions divided by actual controlled emission) for a multi-release single-point,  $\pm 45^{\circ}$  wind sector range. An MRF of less than 1 shows an overall underestimation of emissions while an MRF of greater than 1 shows an overall overestimation of emissions. The dotted blue lines are the lower confidence intervals (CI) and upper CI, 95% confidence intervals.

### 3.2 Aerodynamic Flux Gradient

#### 3.2.1 Single-Release Single-Point

For SRSP emissions, the MRF for AFG was 1.41, 1.67 and 1.30 at  $\pm 45^{\circ}$  wind sector range, for a 112, 56 and 34 sample size at an averaging period of 5, 10 and 15 minutes (Figure 6). At  $\pm 5^{\circ}$  wind sector range, the sample size was 3 at 5-minutes and 0 at 10 and 15-minutes averaging periods, hence, no reasonable quantification results (Supplementary Information Section 3.2.1). Similarly, at  $\pm 10^{\circ}$  wind sector range, the sample size was 7, 1 and 2, at averaging periods of 5, 10 and 15-minutes, respectively (Supplementary Information Section 3.2.1). For the  $\pm 20^{\circ}$  wind sector range, the MRF was 0.75, 0.48 and 1.58 for a sample size of 26, 8 and 4, at averaging periods of 5, 10 and 15-minutes, respectively (Supplementary Information Section 3.2.1). These results show that close-to-stable MRF for ARF is achieved over a wide sector range,  $\pm 45^{\circ}$ .

# $\frac{\text{Aerodynamic Flux Gradient}}{\text{Single-Release Single-Point - }\pm 45^{\circ}}$

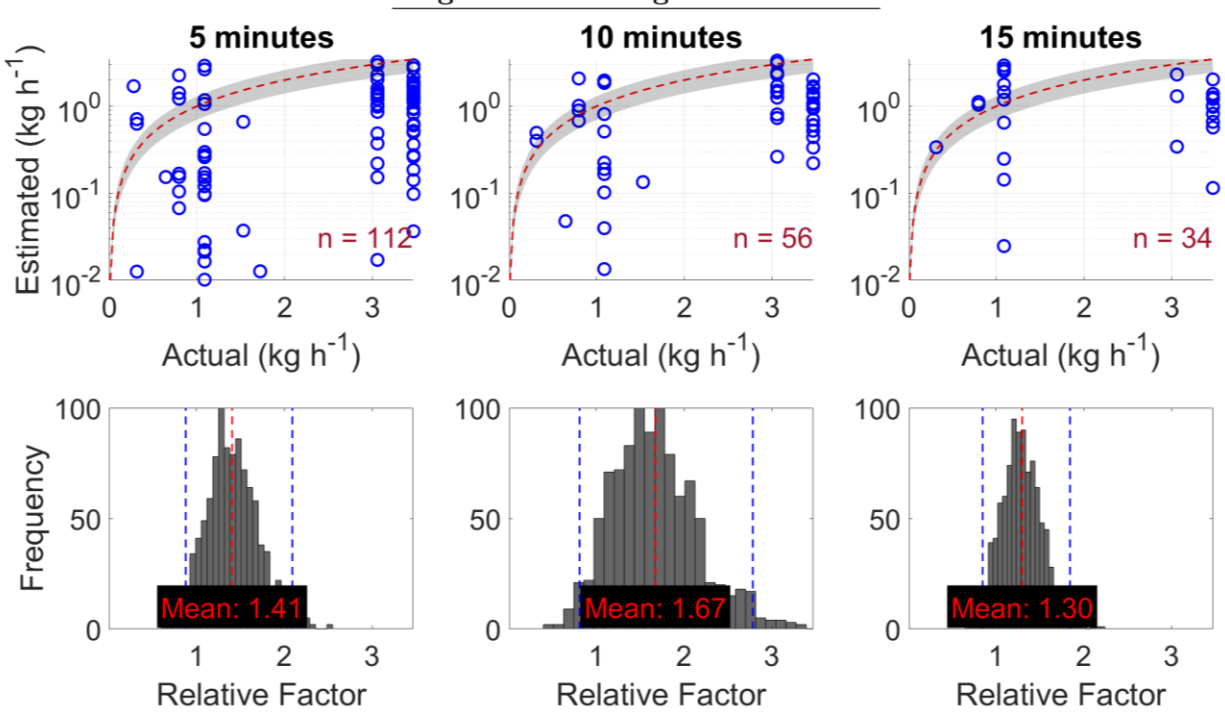


Figure 6. Top plot: Estimated emission vs actual emission (kg h<sup>-1</sup>) for a multi-release single-point at site level,  $\pm 45^{\circ}$  wind sector range. The red dotted line is a 1:1 line based on actual emissions i.e. points below the line are underestimated and above are overestimated emissions. The gray region represents  $\pm 30\%$  of the actual emission. The sample size is n. Bottom plot: A bootstrap of mean relative factor (MRF: estimated emissions divided by actual controlled emission) for a multi-release single-point,  $\pm 45^{\circ}$  wind sector range. An MRF of less than 1 shows an overall underestimation of emissions while an MRF of greater than 1 shows an overall overestimation of emissions. The dotted blue lines are the lower confidence intervals (CI) and upper CI, 95% confidence intervals.

### 3.2.2 Multi-Release Single-Point

For MRSP emissions, generally, the MRF for AFG was between 2 and 9 for all wind sector ranges and averaging periods. The MRF was 3.32, 2.40 and 2.48 at  $\pm 45^{\circ}$  wind sector range, for a 278, 146 and 94 sample size at an averaging period of 5, 10 and 15 minutes (Figure 7). At  $\pm 5^{\circ}$  wind sector range, the MRF was 8.84, 2.51 and 2.93 for a 36, 20 and 13 sample size at 5, 10 and 15-minutes averaging periods, respectively (Supplementary Information Section 3.2.2). At  $\pm 10^{\circ}$  wind sector range, the MRF was 6.12, 2.29 and 2.61 for a 76, 40 and 26 sample size, at averaging periods of 5, 10 and 15-minutes, respectively (Supplementary Information Section 3.2.2). For the  $\pm 20^{\circ}$  wind sector range, the MRF was 5.16, 2.24 and 4.69 for a 142, 74, and 42 sample size, at averaging periods of 5, 10 and 15-minutes, respectively (Supplementary Information Section 3.2.2). These results show that close-to-stable MRF for ARF is achieved for longer-averaging (10 to 15 minutes) and wide sector ranges of  $\pm 45^{\circ}$ .

# 

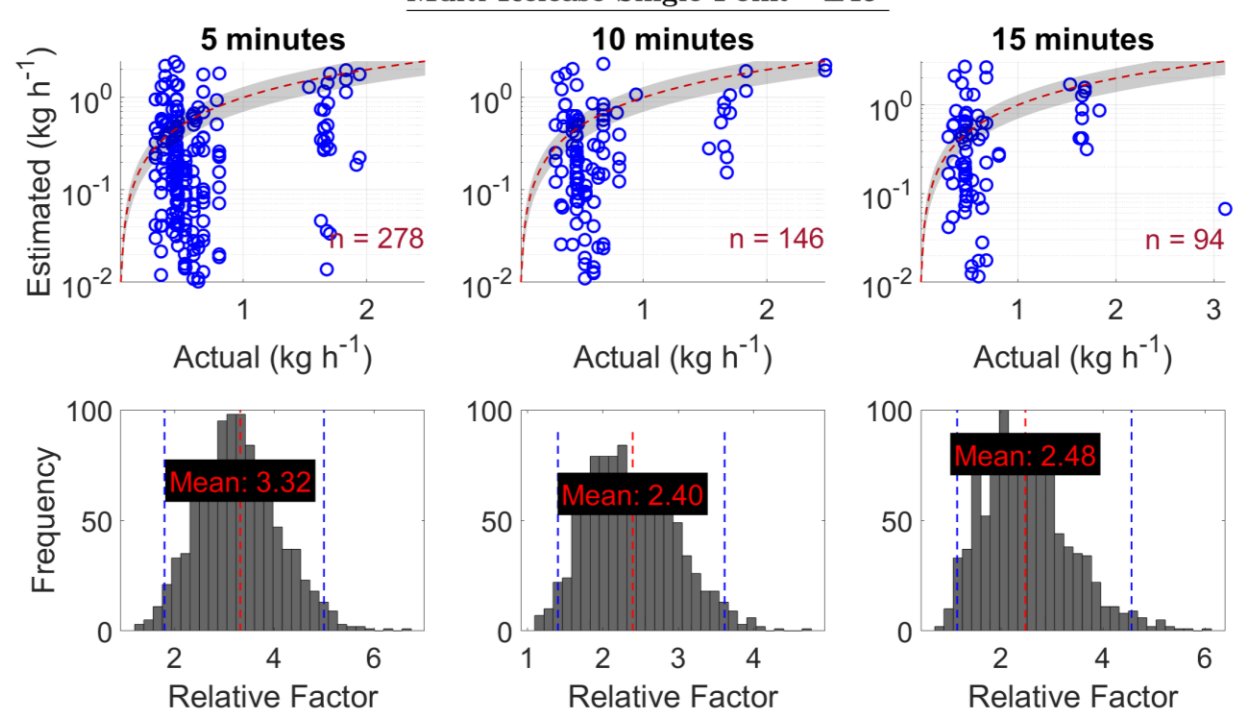


Figure 7. Top plot: Estimated emission vs actual emission (kg h<sup>-1</sup>) for a multi-release single-point at site level,  $\pm 45^{\circ}$  wind sector range. The red dotted line is a 1:1 line based on actual emissions i.e. points below the line are underestimated and above are overestimated emissions. The gray region represents  $\pm 30\%$  of the actual emission. The sample size is n. Bottom plot: A bootstrap of mean relative factor (MRF: estimated emissions divided by actual controlled emission) for a multi-release single-point,  $\pm 45^{\circ}$  wind sector range. An MRF of less than 1 shows an overall underestimation of emissions while an MRF of greater than 1 shows an overall overestimation of emissions. The dotted blue lines are the lower confidence intervals (CI) and upper CI, 95% confidence intervals.

# 3.4 Gaussian Plume Inverse Method

# 3.4.1 Single-Release Single-Point

Generally, the GPIM quantified SRSP emissions between an MRF of 1.85 and 443.54 for all wind sector ranges and averaging periods. The MRF was 2.58, 2.37 and 2.63 for a 79, 41, and 27 sample size, at 5, 10 and 15-minutes averaging period, respectively at  $\pm 10^{\circ}$  wind sector range (Figure 8). At  $\pm 5^{\circ}$  wind sector range, the MRF was 2.26, 1.85 and 3.04 for a sample size of 31, 22 and 17 at 5, 10 and 15-minutes averaging period; and at  $\pm 20^{\circ}$  wind sector range, the MRF was 443.54, 3.36 and 3.14 for 165, 88, and 57 sample size, at averaging periods of 5, 10 and 15-minutes, respectively (Supplementary Information Section 3.3.1). The GPIM MRF is more stable at narrow wind-sector ranges, and over a long averaging period, 10 to 15 minutes.

# Gaussian Plume Inverse Method Single-Release Single-Point - $\pm 10^{\circ}$

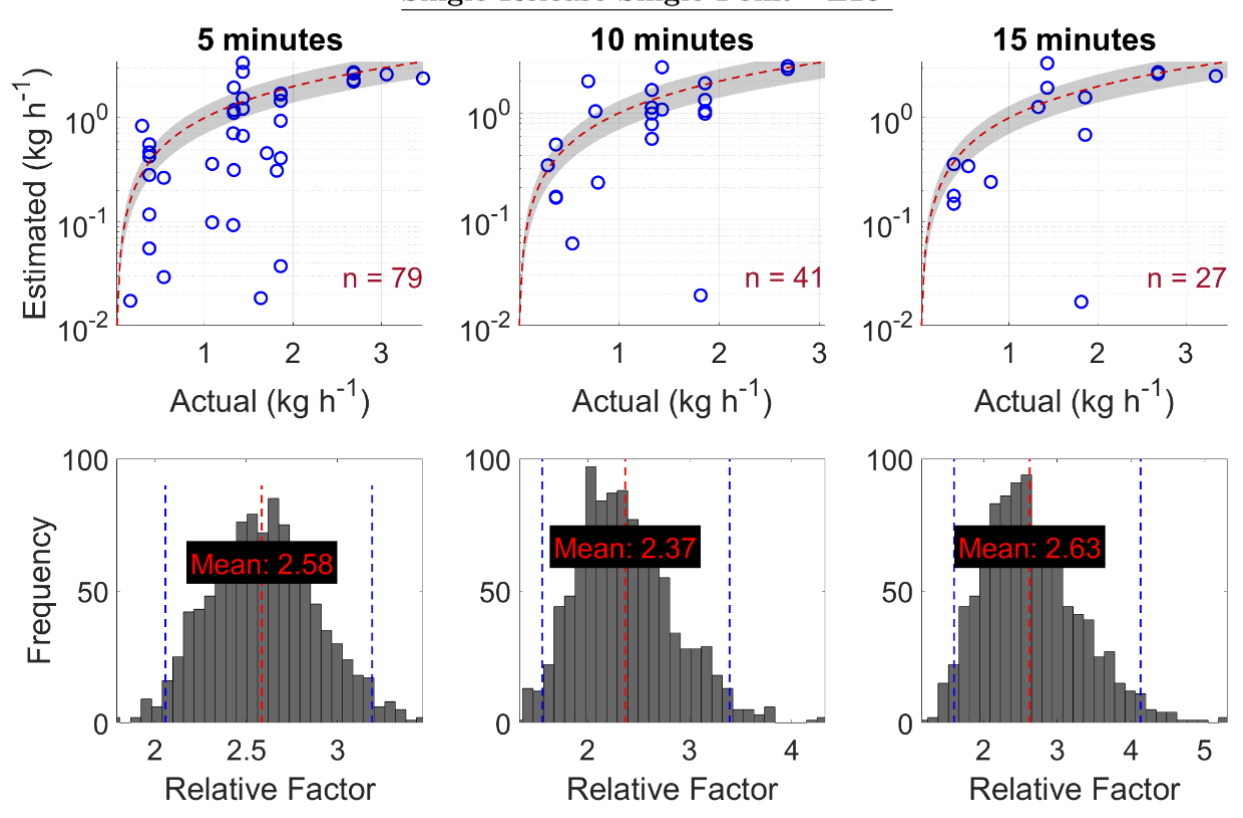


Figure 8. Top plot: Estimated emission vs actual emission (kg h<sup>-1</sup>) for a multi-release single-point at site level,  $\pm 45^{\circ}$  wind sector range. The red dotted line is a 1:1 line based on actual emissions i.e. points below the line are underestimated and above are overestimated emissions. The gray region represents  $\pm 30\%$  of the actual emission. The sample size is n. Bottom plot: A bootstrap of mean relative factor (MRF: estimated emissions divided by actual controlled emission) for a multi-release single-point,  $\pm 45^{\circ}$  wind sector range. An MRF of less than 1 shows an overall underestimation of emissions while an MRF of greater than 1 shows an overall overestimation of emissions. The dotted blue lines are the lower confidence intervals (CI) and upper CI, 95% confidence intervals.

# 3.4.2 Multi-Release Single-Point

The MRF GPIM results for MRSP emissions were between 15.72 and 29.01 for all wind sector ranges and averaging periods. The MRF was 15.72, 24.95 and 16.97 for an 827, 430, and 256 sample size, at 5, 10 and 15-minutes averaging period, respectively at  $\pm 10^{\circ}$  wind sector range (Figure 9). At  $\pm 5^{\circ}$  wind sector range, the MRF was 26.77, 25.04 and 29.01 for a sample size of 398, 189 and 132 sample size at 5, 10 and 15-minutes averaging period; and at  $\pm 20^{\circ}$  wind sector range, the MRF was 18.15, 23.07 and 19.96 for a 1273, 656, and 407 sample size, at averaging periods of 5, 10 and 15-minutes, respectively (Supplementary Information Section 3.3.2). Generally, the GPIM overestimated MSRP emissions by up to a magnitude of 20.

# $\frac{Gaussian\ Plume\ Inverse\ Method}{Multi-Release\ Single-Point}\ -\ \pm 10^{\circ}$

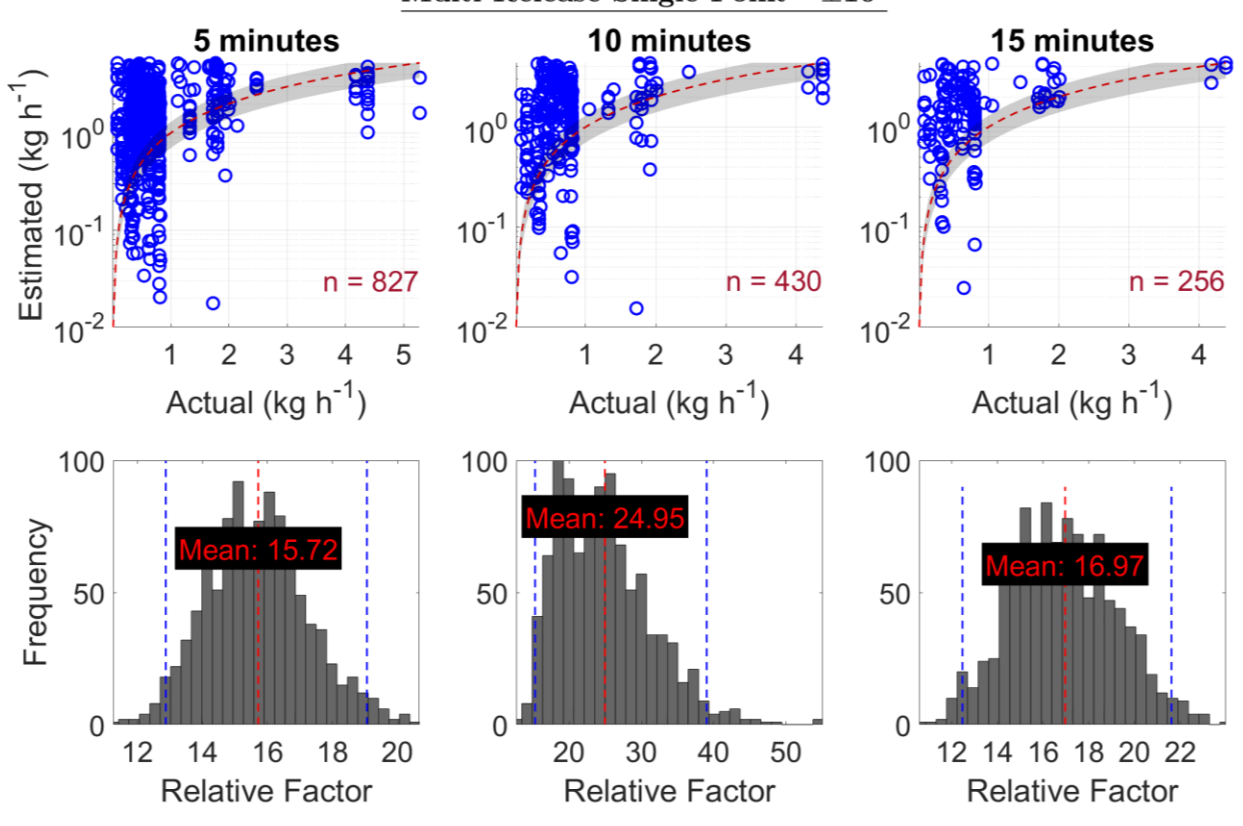


Figure 9. Top plot: Estimated emission vs actual emission (kg h<sup>-1</sup>) for a multi-release single-point at site level,  $\pm 45^{\circ}$  wind sector range. The red dotted line is a 1:1 line based on actual emissions i.e. points below the line are underestimated and above are overestimated emissions. The gray region represents  $\pm 30\%$  of the actual emission. The sample size is n. Bottom plot: A bootstrap of mean relative factor (MRF: estimated emissions divided by actual controlled emission) for a multi-release single-point,  $\pm 45^{\circ}$  wind sector range. An MRF of less than 1 shows an overall underestimation of emissions while an MRF of greater than 1 shows an overall overestimation of emissions. The dotted blue lines are the lower confidence intervals (CI) and upper CI, 95% confidence intervals.

### 3.4 Backward Lagrangian Stochastic Model

# 3.4.1 Single-Release Single-Point

For SRSP emissions, the bLs method estimated emissions between 0.68 and 1.34 MRF. At  $\pm 10^{\circ}$  wind sector range, the MRF was 1.05, 0.80 and 0.86 for 78, 40 and 26 sample size, at 5, 10 and 15-minutes averaging period, respectively (Figure 10). At  $\pm 5^{\circ}$  wind sector range, the MRF was 0.72, 0.68 and 0.82 for a sample size of 31, 22 and 17 at 5, 10 and 15-minutes averaging period; and at  $\pm 20^{\circ}$  wind sector range, the MRF was 1.34, 1.34 and 1.33 for a 131, 70 and 49 sample size, at averaging periods of 5, 10 and 15-minutes, respectively (Supplementary Information Section 3.4.1). Comparing bLs method to GPIM for SRSP emissions as they are both point-source methods, the MRF for bLs was closer 1 indicating higher possibility of correct quantification.

# $\frac{\textbf{Backward Lagrangian Stochastic Model}}{\textbf{Single-Release Single-Point - } \pm 10^{\circ}}$

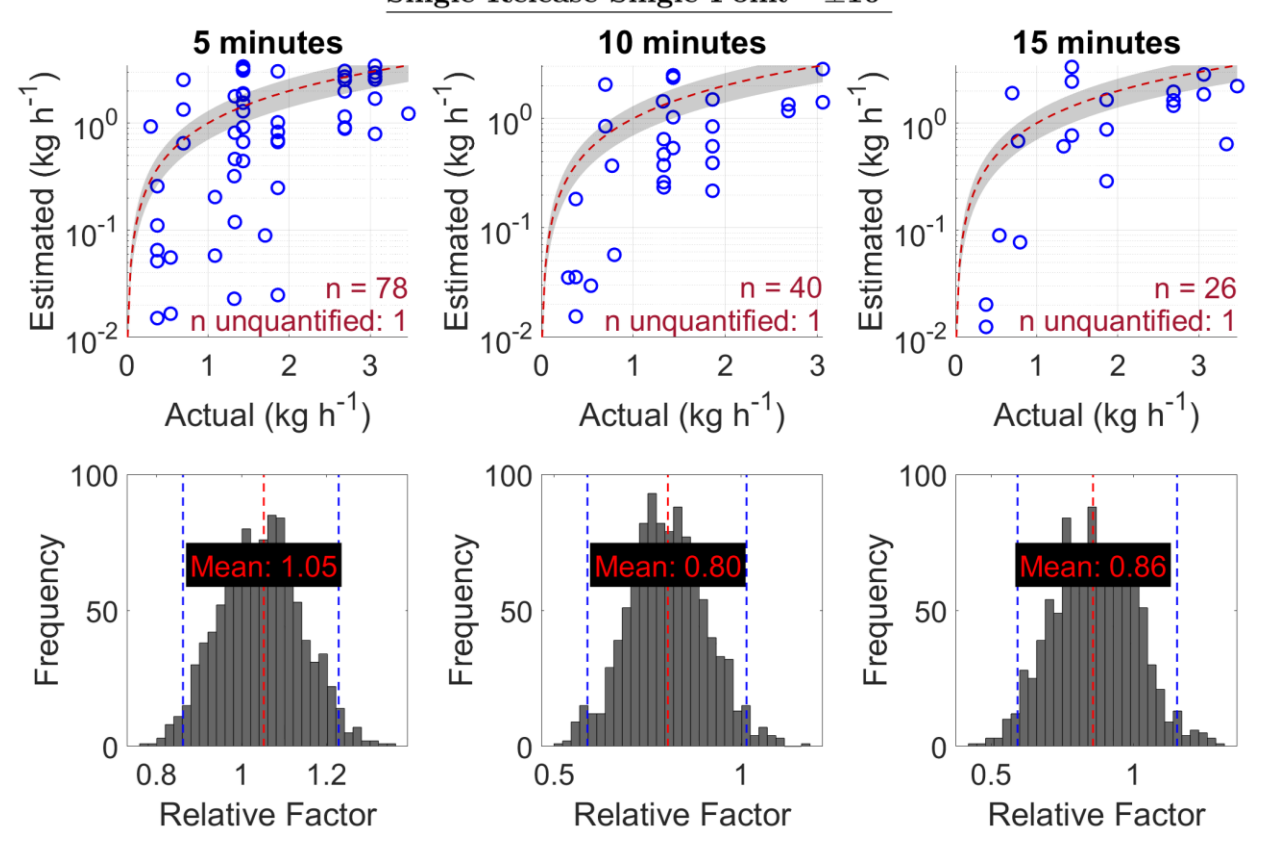


Figure 10. Top plot: Estimated emission vs actual emission (kg h<sup>-1</sup>) for a multi-release single-point at site level,  $\pm 45^{\circ}$  wind sector range. The red dotted line is a 1:1 line based on actual emissions i.e. points below the line are underestimated and above are overestimated emissions. The gray region represents  $\pm 30\%$  of the actual emission. The sample size is n, and "n unquantified" is the number of points WindTrax reported -9999 (i.e. could not quantify). Bottom plot: A bootstrap of mean relative factor (MRF: estimated emissions divided by actual controlled emission) for a multi-release single-point,  $\pm 45^{\circ}$  wind sector range. An MRF of less than 1 shows an overall underestimation of emissions while an MRF of greater than 1 shows an overall overestimation of emissions. The dotted blue lines are the lower confidence intervals (CI) and upper CI, 95% confidence intervals.

### 3.4.2 Multi-Release Single-Point

For MRSP emissions, the bLs method largely overestimated emissions at between an MRF of 3.85 and 12239.20. At  $\pm 10^{\circ}$  wind sector range, the MRF was 411.98, 11958.83 and 3.85 for a 706, 362 and 214 sample size, at 5, 10 and 15-minutes averaging period, respectively (Figure 11). At  $\pm 5^{\circ}$  wind sector range, the MRF was 7.04 and 6.81 and 10 and 15-minutes averaging periods, 186 and 126 sample sizes; and 12239.20 and 5.08 for a 458 and 286 sample size, 10 and 15-minutes averaging period, at  $\pm 20^{\circ}$  wind sector range (Supplementary Information Section 3.4.2). These results show that the bLs model largely overestimated emissions when there were multiple releases at the site level.

# $\frac{ Backward\ Lagrangian\ Stochastic\ Model}{ Multi-Release\ Single-Point\ -\ \pm 10^{\circ}}$

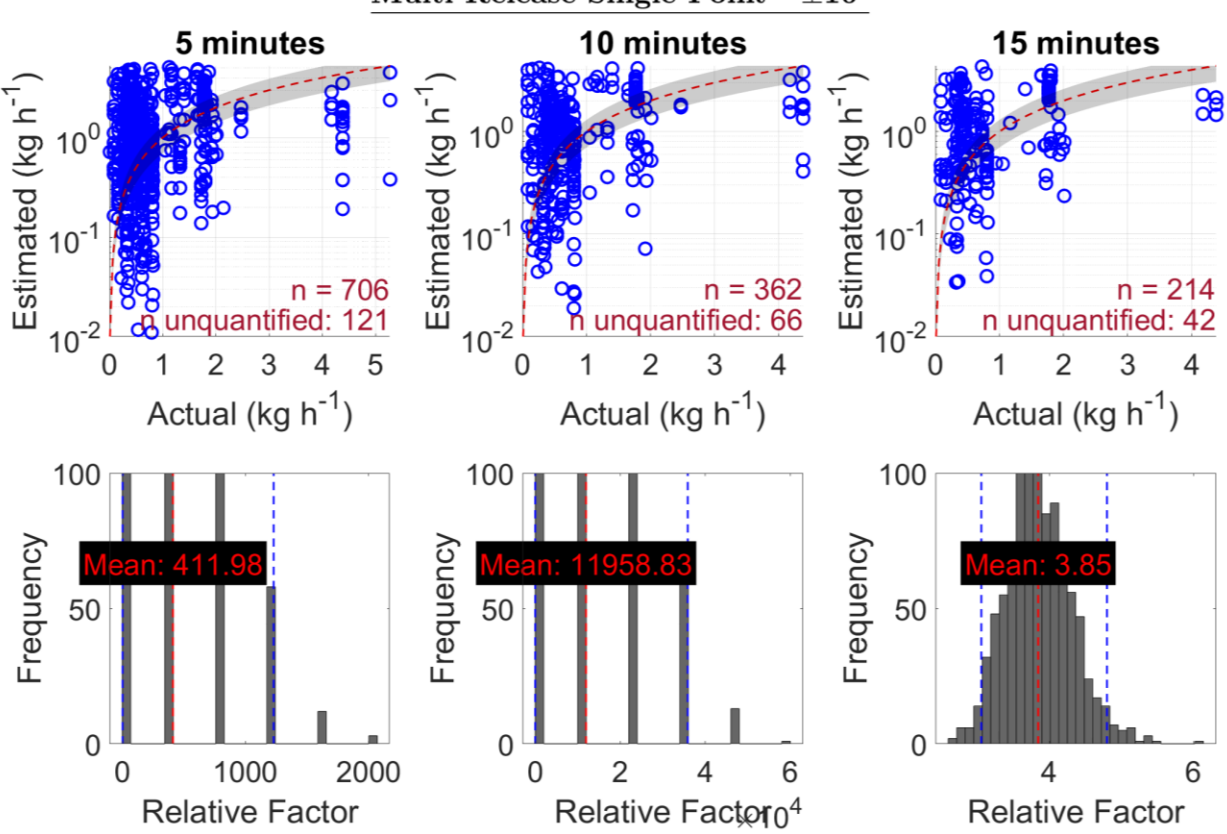


Figure 11. Top plot: Estimated emission vs actual emission (kg h-1) for a multi-release single-point at site level,  $\pm 45^{\circ}$  wind sector range. The red dotted line is a 1:1 line based on actual emissions i.e. points below the line are underestimated and above are overestimated emissions. The gray region represents  $\pm 30\%$  of the actual emission. The sample size is n, and "n unquantified" is the number of points WindTrax reported -9999 (i.e. could not quantify). Bottom plot: A bootstrap of mean relative factor (MRF: estimated emissions divided by actual controlled emission) for a multi-release single-point,  $\pm 45^{\circ}$  wind sector range. An MRF of less than 1 shows an overall underestimation of emissions while an MRF of greater than 1 shows an overall overestimation of emissions. The dotted blue lines are the lower confidence intervals (CI) and upper CI, 95% confidence intervals.

# 4 Discussion

Methane emissions quantification from oil and gas is a complex system comprising of gas emissions from different heights, different locations, encountering aerodynamic obstacles of different sizes, and of varying emissions duration, amongst others. The ability to precisely quantify emissions using data collected by a point sensor, downwind of a source is directly influenced by plume dynamics. The CH<sub>4</sub> plume downwind of a source will change in size and shape in different atmospheric conditions, in open areas versus areas with obstacles, diurnally, and in different seasons (Casal, 2008). In this study, the precision to which downwind methods (closed-path EC, AFG, GPIM and bLs) could quantify the emission rate of point source(s) were tested in different atmospheric conditions (rain, sunny, snow, windy, calm etc.), and aerodynamic scenarios (emissions sources in open areas, behind obstacles, changing atmospheric stability, and day/night). As a result, testing the predicted emission rates to controlled release rates in different

conditions introduced real-world scenarios that have not previously been tested, hence better understanding model uncertainty in the application of quantifying emissions from oil and gas production infrastructure.

# **4.1 Eddy Covariance**

Eddy covariance was tested using a closed-path analyzer, cavity ring-down spectroscopy, with a 3.2 lpm pump flowrate and a 0.4 s gas flow response time. The closed-path EC estimated emissions between a factor of 0.67 and 0.97 for SRSP emissions, and between 1.02 and 2.43 for MRSP emissions at  $\pm 45^{\circ}$  wind sector range (Section 3.1). This was a wider uncertainty in estimated emissions than one reported by Dumortier et al. (2019), who estimated emissions at between 90 and 113% of true emission (~1.5 kg day<sup>-1</sup>) with concentrations between 2 and 3 ppm. Our study tested closed-path EC at emission rates between 0.005 and 8.5 kg h<sup>-1</sup>.

Our study's results were when the data was filtered for frequencies greater than 8 Hz, hence, largely reducing the sampled emissions. The 10 Hz sampling frequency set for this instrument was not a true 10 Hz and this could have been due to the 0.4 gas flow response time that delayed analysis of the drawn air sample in the cavity, or the 3 lpm pump flow rate for a 3 m tubing that might have varied the effective sample turnover rate. The rest of the data were flagged as low quality by Mauder and Foken (2004) (0-1-2 system), which flags based on steady state and well-developed turbulence. This could have been due to low turbulence as experiments were carried out in winter, and instrumentation limitations (low pump flow rate and asynchronous configuration of the gas analyzer and meteorological instrument).

Continuous monitoring requires deployment of multiple sensors which create limitations of cost and requires instrumentation with a wide measurement range as concentrations for oil and gas emissions can range between 0 to 250 ppm, as in this study (Supplementary Information Section 1). The currently available EC instruments have a narrow measurement range (LI-COR LI-7700 open path CH<sub>4</sub> analyzer has a measurement range of 0 to 25 ppm at -25 °C and 0 to 40 ppm at 25°C; PICARRO G2311-f, a closed-path analyzer has an operating range of 0 to 20 ppm). Also, the instrumentation should be environmentally robust and not lab-grade (be able to run smoothly in adverse weather conditions). Given these parameters, market available EC instruments that can currently be deployed in oil and gas are limited. The instrument used in this study is a field instrument (ABB MGGA GLA131 Series has a measurement range of 0 to 100 ppm for CH<sub>4</sub> but can be extended to 0 to 1%).

# 4.2 Aerodynamic Flux Gradient

Overall, the AFG method quantified emissions within an MRF of 1.3 to 1.7 for SRSP emissions and between an MRF of 2.4 and 3.3 for MRSP emissions (Section 3.2). The uncertainties in AFG were higher than EC especially for MRSP emissions but lower than the GPIM and bLs methods. The differences between AFG and EC could have been due to different instrumentation and analytical approaches that limited the exact comparison of the methods i.e. EC data was filtered for frequencies less than 8 Hz, and AFG instrumentations required both analyzers to be running, periods when one analyzer was down, were not tested. To our knowledge, this is the first study to test AFG for point source quantification and results are promising.

Compared to the EC method that requires a very fast analyzer which may be difficult to deploy in oil and gas, the AFG requires at least 2 analyzers sampling at 1 Hz frequency, which is currently possible with the range of sensors available in the market. The main advantage of flux gradient methods (EC and AFG) tested in this study is

that they do not require background control as background CH<sub>4</sub> concentration is a highly variable parameter that cannot be controlled in open air especially when multiple emissions are happening. The AFG method relies on differences in CH<sub>4</sub> concentrations between two heights and this study shows that in complex sites where there are multiple sources, the method quantifies better than the point-source GPIM and bLs methods. The main limitation of the AFG and EC methods for point-source quantification is that when the measurement point is downwind of more than one source in a wind sector range, more than one sonic anemometers are required to estimate the flux of each source for footprint calculation based on Dumortier et al. (2019)'s calculations.

## 4.3 Gaussian Plume Inverse Method

The GPIM method quantified emissions within an MRF of 2.4 and 2.6 for SRSP and between 15.7 and 25 for MRSP emissions (Section 3.3). The GPIM method is a point-source specific quantification approach and works best in open areas, free of obstacles, and when the background concentration is well defined. For multiple emissions, in aerodynamically complex environments, even though the sensor is downwind of a single source based on average wind direction, quantification is complexed by interference from other neighboring sources. The GPIM has previously been reported to quantify emissions within 40.7 and 60% error for a single point-source, (Riddick et al., 2022b). However, GPIM correct quantification has been suggested to be better for longer distances where the plume is well mixed. This is typically a challenge for fence-line sensors that have to be deployed within the facility boundaries where large downwind distances may not be practical.

# 4.3 Backward Lagrangian Stochastic Model

The bLs method quantified emissions within an MRF of 0.8 to 1.05 for SRSP emissions and between 3.85 and 11958.8 MRF for MRSP emissions (Section 3.4). Similarly to the GPIM method, the bLs method used in this study is a point-source specific quantification method that simulates transport of molecules in open area and where the background concentration is defined. In this case, as with the SRSP test scenario, the bLs approach quantified within 20% uncertainty. However, for MRSP emissions, the bLs largely overestimated emissions and this could have been due to the interference of neighboring sources, that even though the measurement point is downwind of a single source, actual plumes are not distinct and model-simulated plumes may not be representative. The point-source bLs approach in WindTrax is also not designed for more than one downwind source.

### 4.4 Implications

In recent years, there has been growing interest and need for accurate CH<sub>4</sub> quantification from oil and gas sites. This is generally done through survey methods and continuous monitoring using fence-line sensors. Continuous monitoring involves having stationary sensors measuring meteorology and CH<sub>4</sub> mixing ratios, which are then used to infer emission rates. For point sources, downwind methods such as the Gaussian plume inverse method have been widely used, especially for survey quantification. Continuous monitoring is relatively new but fast growing. This study's design replicated a continuous monitoring setup's downwind deployment distance, range of typical emission rates, emissions heights, and meteorological data acquisition.

Oil and gas point sources could either be single emissions or multiple emissions occurring concurrently. In cases of multiple emissions with more than one release point being upwind, the Gaussian model and the backward Lagrangian stochastic models are limited, as they can only quantify one source at a time; and interference from

neighboring emissions affects the underlying principles of dispersion on which these models were developed. As a result, flux quantification models used in other applications such as eddy covariance and aerodynamic flux gradient have been proposed as the solution. This study's results show that generally reasonable quantification estimates are achieved with flux approaches (eddy covariance and aerodynamic flux gradient), but these methods require more instrumentation effort (fast sampling analyzer for eddy covariance, and multiple collocated sensors for aerodynamic flux gradient). Even though the widely applied Gaussian plume inverse method and the backward Lagrangian stochastic models are widely used for single-point emissions, this study shows aerodynamic complexities, the difficulty in defining the background, and interference from neighboring sources challenge the application of these models for fence-line continuous monitoring. This study recommends more testing of flux quantification models for oil and gas quantification as they could improve emissions quantification for leak repair prioritization and methane reporting.

# 530 Author contributions

519

520

521

522

523

524

525

526

527

528

529

- Mercy Mbua: Conceptualization, Data curation, Methodology, Formal analysis, Investigation, Writing original draft,
- Review, and Editing. Stuart N. Riddick: Conceptualization, Methodology, Review, Editing, Project Administration,
- 533 Supervision, and Funding Acquisition. Elijah Kiplimo: Investigation, Review, and Editing. Kira B. Shonkwiler:
- Review and Editing. Anna Hodshire: Review and Editing. Daniel Zimmerle: Review, Editing, Funding acquisition,
- and Project administration.

# 536 Declaration of competing interest

- The authors declare that they have no known competing financial interests or personal relationships that could have
- appeared to influence the work reported in this paper.

# 539 Acknowledgment

- This work is funded by the Office of Fossil Energy and Carbon Management within the Department of Energy as part
- of the Site-Air-Basin Emissions Reconciliation (SABER) Project #DE-FE0032288. Any opinions, findings,
- 542 conclusions, or recommendations expressed herein are those of the authors and do not necessarily reflect the views of
- those providing technical input or financial support. The trade names mentioned herein are merely for identification
- purposes and do not constitute endorsement by any entity involved in this study. The authors also thank Ryan Brouwer,
- Daniel Fleischmann, Ryan Buenger, and Wendy Hartzell for their assistance.

# 546 Data availability

- Data sets for this research are available in the in-text data citation reference: Mbua, Mercy; Riddick, Stuart N.;
- Kiplimo, Elijah et al. (Forthcoming 2025). Evaluating the feasibility of using downwind methods to quantify point
- 549 source oil and gas emissions using continuous monitoring fence-line sensors [Dataset].
- Dryad. https://doi.org/10.5061/dryad.hhmgqnkss

# References

551

- Bell, C., Ilonze, C., Duggan, A., Zimmerle, D., 2023. Performance of continuous emission monitoring solutions
- 553 under a single-blind controlled testing protocol. Environ. Sci. Technol. 57, 5794–5805.
- 554 https://doi.org/10.1021/acs.est.2c09235.

- Brown, J.A., Harrison, M.R., Rufael, T., Roman-White, S.A., Ross, G.B., George, F.C., Zimmerle, D., 2023.
- Informing methane emissions inventories using facility aerial measurements at midstream natural gas
- facilities. Environ. Sci. Technol. 57, 14539–14547. https://doi.org/10.1021/acs.est.3c01321.
- Carbon Mapper Science & Technology [WWW Document], n.d. URL https://carbonmapper.org/work/science (accessed 2.18.25).
- Casal, J., 2008. Chapter 6 Atmospheric dispersion of toxic or flammable clouds, in: Industrial Safety Series.
- 561 Elsevier, pp. 195–248. https://doi.org/10.1016/S0921-9110(08)80008-0.
- Colorado State University, 2021. Mechanistic Emission Estimation Tool (MEET) [WWW Document]. Energy Inst.
- URL https://energy.colostate.edu/mechanistic-air-emissions-simulator/ (accessed 2.26.24).
- Conrad, B.M., Tyner, D.R., Johnson, M.R., 2023. Robust probabilities of detection and quantification uncertainty
- for aerial methane detection: Examples for three airborne technologies. Remote Sens. Environ. 288,
- 566 113499. https://doi.org/10.1016/j.rse.2023.113499.
- 567 Crenna, B., 2006. An introduction to WindTrax. http://thunderbeachscientific.com/downloads/introduction.pdf.
- Day, R.E., Emerson, E., Bell, C., Zimmerle, D., 2024. Point sensor networks struggle to detect and quantify short
- controlled releases at oil and gas sites. Sensors 24, 2419. https://doi.org/10.3390/s24082419.
- 570 Denmead, O.T., 2008. Approaches to measuring fluxes of methane and nitrous oxide between landscapes and the
- $571 \hspace{1.5cm} atmosphere. \hspace{0.1cm} Plant \hspace{0.1cm} Soil \hspace{0.1cm} 309, \hspace{0.1cm} 5-24. \hspace{0.1cm} \hspace{0.1cm}$
- 572 Dumortier, P., Aubinet, M., Lebeau, F., Naiken, A., Heinesch, B., 2019. Point source emission estimation using
- eddy covariance: Validation using an artificial source experiment. Agric. For. Meteorol. 266–267, 148–
- 574 156. https://doi.org/10.1016/j.agrformet.2018.12.012.
- Foken, Th., Wichura, B., 1996. Tools for quality assessment of surface-based flux measurements. Agric. For.
- 576 Meteorol. 78, 83–105. https://doi.org/10.1016/0168-1923(95)02248-1.
- Foster-Wittig, T.A., Thoma, E.D., Albertson, J.D., 2015. Estimation of point source fugitive emission rates from a
- single sensor time series: A conditionally-sampled Gaussian plume reconstruction. Atmos. Environ. 115,
- 579 101–109. https://doi.org/10.1016/j.atmosenv.2015.05.042.
- Fratini, G., Ibrom, A., Arriga, N., Burba, G., Papale, D., 2012. Relative humidity effects on water vapour fluxes
- measured with closed-path eddy-covariance systems with short sampling lines. Agric. For. Meteorol. 165,
- 582 53–63. https://doi.org/10.1016/j.agrformet.2012.05.018.
- Horst, T.W., Lenschow, D.H., 2009. Attenuation of scalar fluxes measured with spatially-displaced sensors.
- 584 Boundary-Layer Meteorology. 130, 275–300. https://doi.org/10.1007/s10546-008-9348-0.
- Hsieh, C.-I., Katul, G., Chi, T., 2000. An approximate analytical model for footprint estimation of scalar fluxes in
- thermally stratified atmospheric flows. Adv. Water Resour. 23, 765–772. https://doi.org/10.1016/S0309-
- 587 1708(99)00042-1.
- Ilonze, C., Emerson, E., Duggan, A., Zimmerle, D., 2024. Assessing the progress of the performance of continuous
- monitoring solutions under a single-blind controlled testing protocol. Environ. Sci. Technol. 58, 10941–
- 590 10955. https://doi.org/10.1021/acs.est.3c08511.

- Johnson, M.R., Tyner, D.R., Szekeres, A.J., 2021. Blinded evaluation of airborne methane source detection using
- Bridger Photonics LiDAR. Remote Sens. Environ. 259, 112418. https://doi.org/10.1016/j.rse.2021.112418.
- Kamp, J.N., Häni, C., Nyord, T., Feilberg, A., Sørensen, L.L., 2020. The aerodynamic gradient method: implications of non-simultaneous measurements at alternating heights. Atmosphere 11, 1067.
- 595 https://doi.org/10.3390/atmos11101067.
- Kljun, N., Calanca, P., Rotach, M.W., Schmid, H.P., 2015. A simple two-dimensional parameterisation for Flux Footprint Prediction (FFP). Geosci. Model Dev. 8, 3695–3713. https://doi.org/10.5194/gmd-8-3695-2015
- Kormann, R., Meixner, F.X., 2001a. An analytical footprint model for non-neutral stratification. Boundary-Layer Meteorology. 99, 207–224. https://doi.org/10.1023/A:1018991015119.
- LICOR, 2025. EddyPro\_Manual\_12025.pdf | Powered by Box [WWW Document]. URL https://licor.app.boxenterprise.net/s/lium2zmwm6hl36yz9bu4 (accessed 2.14.25).
- 602 LI-COR, Nebraska, USA, n.d. EddyPro 7 | Software Downloads [WWW Document]. URL 603 https://www.licor.com/support/EddyPro/software.html (accessed 1.30.25).
- Mauder, M., Foken, T., 2004. Documentation and instruction manual of the eddy covariance software package TK2. https://epub.uni-bayreuth.de/id/eprint/884/1/ARBERG026.pdf.
- METEC, 2025. METEC | Colorado State University [WWW Document]. URL https://metec.colostate.edu/607 (accessed 2.18.25).
- Moncrieff, J., Clement, R., Finnigan, J., Meyers, T., 2005. Averaging, Detrending, and Filtering of Eddy Covariance
   Time Series, in: Lee, X., Massman, W., Law, B. (Eds.), Handbook of Micrometeorology, Atmospheric and
   Oceanographic Sciences Library. Kluwer Academic Publishers, Dordrecht, pp. 7–31.
   https://doi.org/10.1007/1-4020-2265-4\_2.
- Morin, T.H., 2019. Advances in the eddy covariance approach to CH<sub>4</sub> monitoring over two and a half decades. J. Geophys. Res. Biogeosciences 124, 453–460. https://doi.org/10.1029/2018JG004796.
- Nemitz, E., Mammarella, I., Ibrom, A., Aurela, M., Burba, G.G., Dengel, S., Gielen, B., Grelle, A., Heinesch, B.,
  Herbst, M., Hörtnagl, L., Klemedtsson, L., Lindroth, A., Lohila, A., McDermitt, D.K., Meier, P., Merbold,
  L., Nelson, D., Nicolini, G., Nilsson, M.B., Peltola, O., Rinne, J., Zahniser, M., 2018. Standardisation of
  eddy-covariance flux measurements of methane and nitrous oxide. Int. Agrophysics 32, 517–549.
- https://doi.org/10.1515/intag-2017-0042.
- Polonik, P., Chan, W.S., Billesbach, D.P., Burba, G., Li, J., Nottrott, A., Bogoev, I., Conrad, B., Biraud, S.C., 2019.

  Comparison of gas analyzers for eddy covariance: Effects of analyzer type and spectral corrections on fluxes. Agric. For. Meteorol. 272–273, 128–142. https://doi.org/10.1016/j.agrformet.2019.02.010.
- Querino, C.A.S., Smeets, C.J.P.P., Vigano, I., Holzinger, R., Moura, V., Gatti, L.V., Martinewski, A., Manzi, A.O.,
   De Araújo, A.C., Röckmann, T., 2011. Methane flux, vertical gradient and mixing ratio measurements in a
   tropical forest. Atmospheric Chem. Phys. 11, 7943–7953. https://doi.org/10.5194/acp-11-7943-2011.
- Rey-Sanchez, C., Arias-Ortiz, A., Kasak, K., Chu, H., Szutu, D., Verfaillie, J., Baldocchi, D., 2022. Detecting hot spots of methane flux using footprint-weighted flux maps. J. Geophys. Res. Biogeosciences 127, e2022JG006977. https://doi.org/10.1029/2022JG006977.

- Riddick, S.N., Ancona, R., Cheptonui, F., Bell, C.S., Duggan, A., Bennett, K.E., Zimmerle, D.J., 2022a. A
  cautionary report of calculating methane emissions using low-cost fence-line sensors. Elem. Sci. Anthr. 10,
  00021. https://doi.org/10.1525/elementa.2022.00021.
- Riddick, S.N., Cheptonui, F., Yuan, K., Mbua, M., Day, R., Vaughn, T.L., Duggan, A., Bennett, K.E., Zimmerle,
- D.J., 2022b. Estimating regional methane emission factors from energy and agricultural sector sources
- using a portable measurement system: Case study of the Denver–Julesburg basin. Sensors 22, 7410.
- https://doi.org/10.3390/s22197410.
- Riddick, S.N., Mauzerall, D.L., 2023. Likely substantial underestimation of reported methane emissions from
  United Kingdom upstream oil and gas activities. Energy Environ. Sci. 16, 295–304.
- https://doi.org/10.1039/D2EE03072A.
- Riddick, S.N., Mbua, M., Anand, A., Kiplimo, E., Santos, A., Upreti, A., Zimmerle, D.J., 2024a. Estimating total methane emissions from the Denver-Julesburg basin using bottom-up approaches. Gases 4, 236–252.
- 640 https://doi.org/10.3390/gases4030014.
- Riddick, S.N., Mbua, M., Santos, A., Hartzell, W., Zimmerle, D.J., 2024b. Potential underestimate in reported bottom-up methane emissions from oil and gas operations in the Delaware basin. Atmosphere 15, 202.
- 643 https://doi.org/10.3390/atmos15020202.
- Tagliaferri, F., Invernizzi, M., Capra, F., Sironi, S., 2023. Validation study of WindTrax reverse dispersion model coupled with a sensitivity analysis of model-specific settings. Environ. Res. 222, 115401.
- 646 https://doi.org/10.1016/j.envres.2023.115401.
- 647 US EPA, OAR, 2023. Natural gas and petroleum systems in the GHG inventory: Additional information on the 648 1990-2021 GHG inventory (published April 2023) [WWW Document]. URL
- https://www.epa.gov/ghgemissions/natural-gas-and-petroleum-systems-ghg-inventory-additional-information-1990-2021-ghg (accessed 5.6.24).
- Vickers, D., Mahrt, L., 1997. Quality control and flux sampling problems for tower and aircraft data. J. Atmospheric Ocean. Technol. 14, 512–526. https://doi.org/10.1175/1520-0426(1997)014<0512:QCAFSP>2.0.CO;2.
- Vogel, E., Davis, K.J., Wu, K., Miles, N.L., Richardson, S.J., Gurney, K.R., Monteiro, V., Roest, G.S., Kenion,
- H.C.R., Horne, J.P., 2024. Using eddy-covariance to measure the effects of COVID-19 restrictions on CO<sub>2</sub> emissions in a neighborhood of Indianapolis, IN. Carbon Manag. 15, 2365900.
- https://doi.org/10.1080/17583004.2024.2365900.
- WindTrax 2.0, n.d. thunder beach scientific [WWW Document]. URL http://www.thunderbeachscientific.com/ (accessed 1.31.25).
- Xu, L., Lin, X., Amen, J., Welding, K., McDermitt, D., 2014. Impact of changes in barometric pressure on landfill
   methane emission. Glob. Biogeochem. Cycles 28, 679–695. https://doi.org/10.1002/2013GB004571
- Zimmerle, D., Dileep, S., Quinn, C., 2024. Unaddressed uncertainties when scaling regional aircraft emission surveys to basin emission estimates. Environ. Sci. Technol. 58, 6575–6585.
- https://doi.org/10.1021/acs.est.3c08972.

664